Chapter 7
Development of an *in-situ* Sensor for Real-time Geometrical Inspection in Additive Manufacturing

Howard Zheng, Anthony Salerni and Cosme Furlong

Abstract Real-time measurements in additive manufacturing (AM) are essential for quality control, enabling the early defect detection in critical parameters such as surface contours, subsurface features, and in certain cases the presence of contaminants. Without real-time monitoring, manufacturing inconsistencies, including shape irregularities and chemical impurities, can compromise part quality leading to part failure and waste. To address this challenge, this paper presents the development of a miniaturized, non-contact, full-field surface sensor for real-time AM monitoring *in-situ*. The development follows a two-stage process: first, a testing platform is designed to replicate high-performance AM fabrication conditions, and second, design constraints are identified to establish integration specifications. The sensor employs a structured light projection system using parallel fringes with a stereo-camera setup, utilizing a phase-to-height look-up table to achieve near-video framerate shape recovery. Performance evaluation using USAF targets and NIST-traceable gauges demonstrates spatial and measuring resolutions of 60 μm and 50 μm, respectively, validating its capability for defect detection and quality control. During operation, the sensor continuously acquires surface geometry data for each printed layer, enabling the creation of a high-resolution digital representation of the AM part. Future efforts will focus on integrating machine learning algorithms for automated compensation, further enhancing fabrication accuracy and process efficiency.

Keywords Additive manufacturing · Fringe projection · *In-situ* measurements · Sensor miniaturization · Smart manufacturing

Introduction

In the evolving landscape of manufacturing, accurate and reliable fabrication processes are essential. Recent advancements in additive manufacturing (AM) have enabled the production of components with complex geometries and higher tolerances, spurring interest in the development of real-time, *in-situ* sensors with a range of measurement modalities. Beyond surface contours, such sensors can capture subsurface defects and monitor chemical impurities in real-time, ensuring comprehensive quality assessments throughout the fabrication process. These wide-ranging measurement capabilities are crucial for maintaining part integrity and optimizing quality control across the entire fabrication processes of AM components. By detecting irregularities at an early stage, *in-situ* monitoring can significantly reduce material waste, improve production efficiency, and enhance the overall reliability of AM-produced parts.

Traditional *ex-situ* inspection methods, such as coordinate-measuring machines and ultrasonic inspection, provide precise measurements of the surface and subsurface features, but only after fabrication is completed. This post-process evaluation results in delayed defect detection, increased production costs, and limited opportunities for corrective actions. In contrast, *in-situ* inspection offers real-time monitoring, enabling early identification of anomalies, and generates an evolving digital representation of the AM part during fabrication. However, designing a miniaturized, non-invasive *in-situ* sensor comes with technical challenges, including achieving high spatial and temporal resolutions, avoiding interference with the AM processes, and ensuring compatibility with various printing environments. Furthermore, the integration of data mining techniques and machine-learning (ML) algorithms enhances the potential of *in-situ* sensing by enabling the use of quantitative

Howard Zheng · Anthony Salerni · Cosme Furlong
Center for Holographic Studies and Laser micro-mechaTronics (CHSLT), Mechanical & Materials Engineering Department, Worcester Polytechnic Institute, Worcester, MA 01609
e-mail: hzheng3@wpi.edu; asalerni72@wpi.edu; cfurlong@wpi.edu

Chi-Hung Hwang et al. (eds.), *Advancement of Optical Methods & Digital Image Correlation in Experimental Mechanics, Vol. 2*, Conference Proceedings
of the Society for Experimental Mechanics Series, https://doi.org/10.13052/97887-438-0828-2_7

measurements to dynamically optimize fabrication parameters. For instance, ML-based systems can automatically adjust print speed, bed temperature, and extrusion rate to compensate for detected irregularities, paving the way for intelligent, adaptive manufacturing processes.

This paper focuses on surface shape measurements and presents progress in assembling a testing platform that replicates AM printing conditions and identifying design constraints that establish integration specifications. Preliminary results, including real-time measurements stitching, are presented, as well as the spatial and temporal resolutions achieved.

Methodology

To properly evaluate the performance of the surface shape sensor, a testing platform is first assembled. This testing platform is designed to replicate AM printing conditions similar to those of a high-performance AM system. The specifications of the testing platform are determined based on the parameters of the targeted AM system, such as the resolution and travelling speed in *x, y,* and *z* axes. Other key optical design (e.g., working distance, illumination wavelength, and field-of-view) are also defined by the constraints of the AM system. The testing platform also incorporates replicas of key structures from the AM system. This allows the sensor's fixtures to be designed around these structures for seamless integration into the AM environment with minimal obstruction to the printing process.

Based on the design constraints identified through construction of the testing platform, a non-invasive, miniaturized surface shape sensor are designed. A structured light fringe projection (FP) system with parallel fringes is employed for surface shape reconstruction. Major components of the FP system include an object of interest, a projector for fringe projection, and a camera to capture the distorted fringe pattern. The three components form a triangulation geometry as shown in Figure 1, and the full field depth information can be recovered via the phase-to-height relationship [1], given by equation

$$\overline{MM'} = \frac{L\Omega}{2\pi f_o D}, \tag{1}$$

where $\overline{MM'}$ is the height of the object at position (*x,y*), L is the distance from the projector's pupil to a reference plane, D is the distance from the projector's pupil to the camera's pupil, f_o is the spatial frequency of the projected fringes, and Ω is

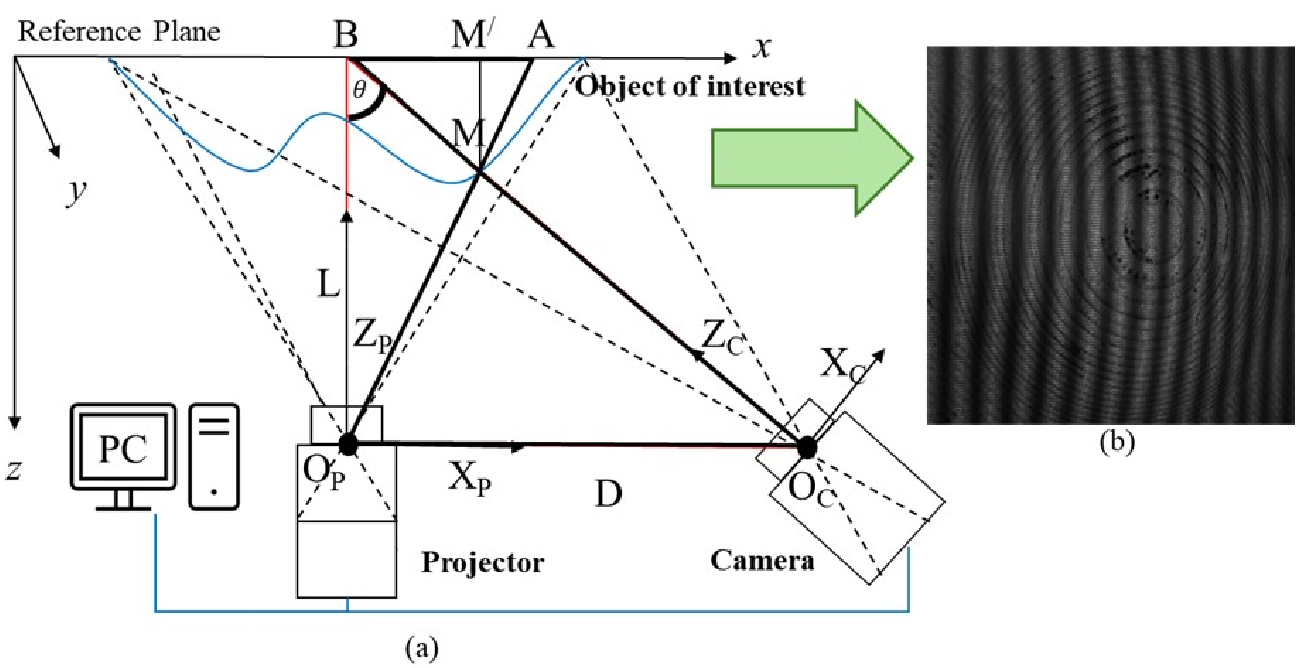

Fig. 1 Fringe projection methodology setup using triangulation principle: (a) schematic of fringe projection system showing the triangulation geometry of the object, projector, and camera; and (b) representative fringe projection pattern on an object of interest.

the optical phase carrying the shape information. The optical phase, Ω, can be extracted via phase-stepping, Fourier domain analysis, or sampling Moiré method [2–5]. However, due to the nature of phase calculation using inverse tangent function, the phase map may contain 2π discontinuities that must be unwrapped before depth can be computed. Phase unwrapping can be done using various methods, including temporal phase unwrapping, quality-guided phase unwrapping, and direct phase-to-height look-up tables [6–8]. For the proposed miniaturized sensor, the direct phase-to-height technique is used because it offers significantly faster computation than the other methods [9].

Realization of Testing Platform and Surface Sensor

Testing platform

Realization of the dynamic testing platform begins with matching both the dynamic and structural criteria of the intended AM system. Dynamic criteria involve matching the fabrication speed and acceleration of the AM system, as well as its movement resolutions along each axis. Structural criteria require the testing platform to have an identical print-head fixture to establish design constraints for seamless integration of the surface sensor. Figure 2 shows a representative FDM-type AM printer, and the realized testing platform constructed around these dynamic and structural criteria. To satisfy the dynamic requirements, the testing platform employs motorized x-y stages that can reach speed up to 200 mm/s with a resolution of 2.5 μm. The platform must also be controllable via G-code, similar to a standard AM system. Structurally, the platform provides a fixture to attach the surface sensor such that the sensor does not interfere with the printing process. A mock print nozzle is attached to the platform to simulate the obstacle presented by an actual AM print-head.

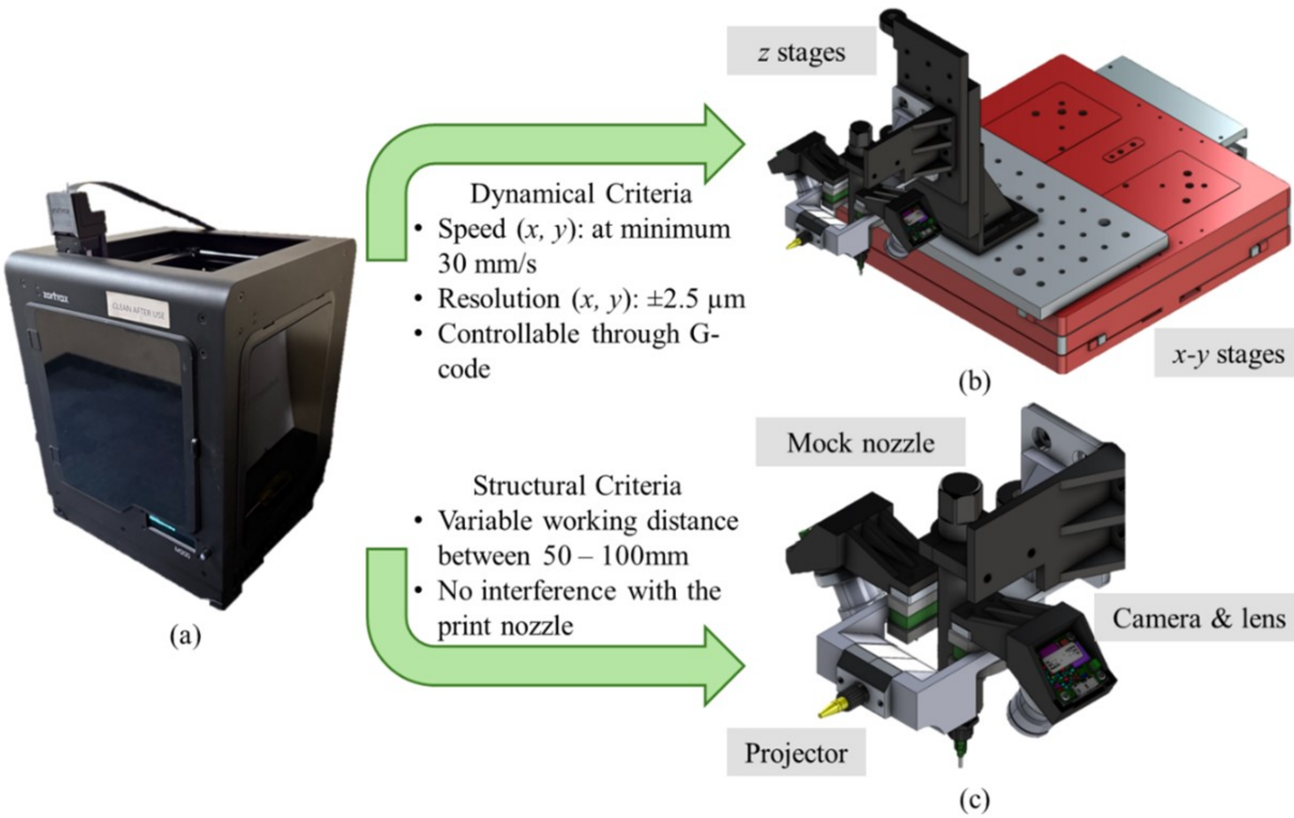

Fig. 2 Schematic illustrating the realization of testing platform by matching the AM system's dynamic and structural criteria: (a) representative FDM-type AM system; (b) testing platform with high-speed, high-precision motorized stages; and (c) replicated print-head with added imaging optics, projectors, and a mocked print nozzle to simulate obstacle in actual AM processes.

Real-time in-situ surface sensor

One major obstacle in applying FP setup for real-time AM measurement is the interference from the printing nozzle. In a conventional FP arrangement, the projector would occupy the same position as the printing nozzle, an obvious conflict. Therefore, the projection path needs to be redirected and rescaled from a different angle to avoid collision with the nozzle. Figure 3 shows the optical design and implementation of such an off-axis projection system. The illumination is introduced from a direction perpendicular to the nozzle, and a biconic mirror together with a biconcave lens are used to redirect and rescale the fringe projection to the appropriate size on the reference plane.

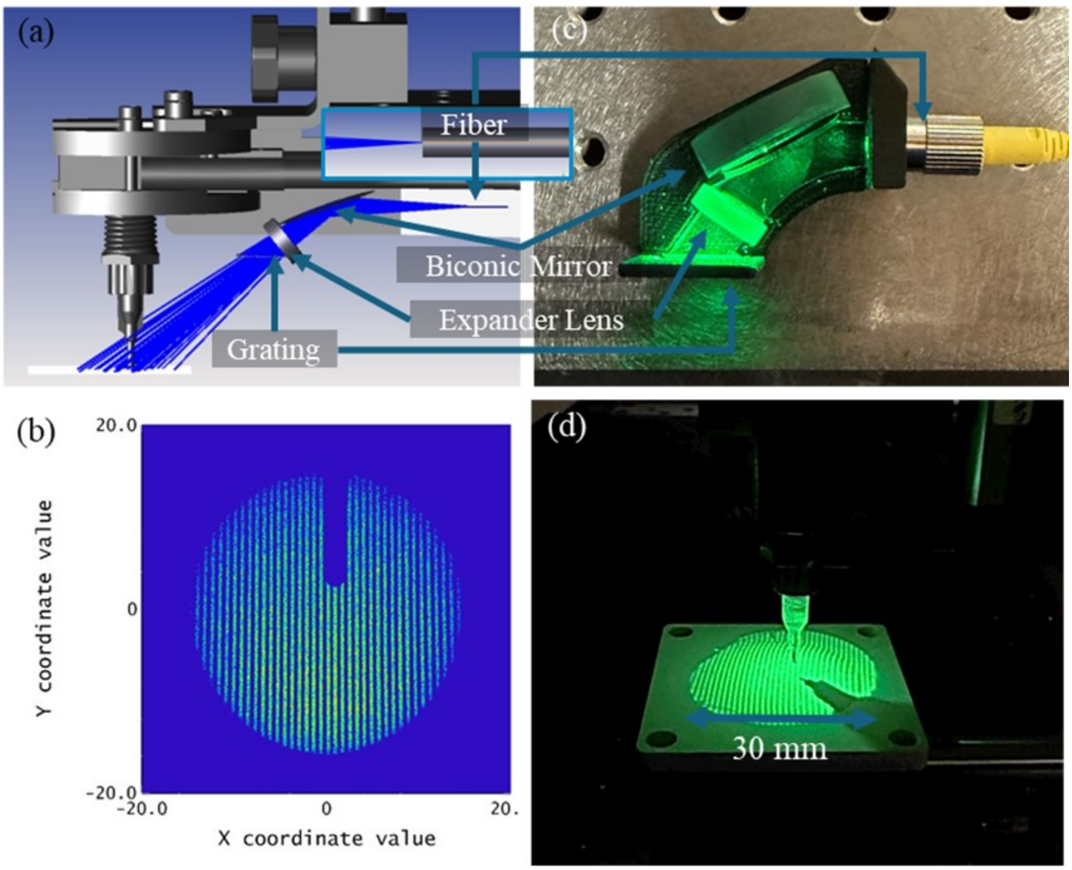

Fig. 3 Design and implementation of the off-axis fringe projection system using a biconic mirror and biconcave expander lens: (a) optical design (Zemax simulation) to obtain the parameters required to redirect and rescale the fringes at the reference plane; (b) simulated projection output accounting for the shadowing effect of the nozzle; (c) physical realization of the off-axis fringe projection system; and (d) implementation of the system shown in (c).

To miniaturize the overall sensor setup, board-level cameras with low profile lens are used. Table 1 provides key parameters of the camera and lens used in the observation system. The selected board-level cameras included general purpose input/output (GPIO) channels that can be configured for stroboscopic imaging, thereby reducing motion blur that would otherwise introduced noise during real-time surface measurements.

Table 1 A list of the camera and lens used in the observation system with relevant parameters

Camera	Lens
Basler daA1920-160um	M12-threaded Lens
2.3 MP full resolution	50° FOV
160 frames per second maximum	6 mm focal length
$30 \times 30 \times 20$ mm^3	$16 \times 16 \times 10$ mm^3
15 grams	7 grams

Representative 3D Reconstruction and Stitching

The spatial and measuring capabilities of the surface sensor are validated using a USAF target and a custom-made NIST traceable target. Figure 4 shows the NIST traceable target and its sinusoidal surface profile design. The sinusoidal NIST target is designed to have a peak-to-peak depth of 0.5 mm and a period of 5 mm; these parameters are chosen based on the project sponsor requirements. Figure 5 shows an image of the USAF target captured with the Basler daA1920-160um camera using the 50° FOV lens at a working distance of 100 mm, and the corresponding 3D reconstruction of the sinusoidal NIST traceable target. The characterized spatial (*x, y*) resolution is approximately 62.5 μm and the measuring (*z*) resolution is approximately 50 μm. Figure 6 illustrates a representative surface measurement stitching result with the sensor operating in real time under a 120 mm/s motion of the testing platform. In figure 6, panels (a)-(d) shows small-area surface measurements at four different time instances, each outlined in a different color; panel (e) shows the stitched single-layer measurements, with outlines corresponding to the colored areas from (a)-(d).

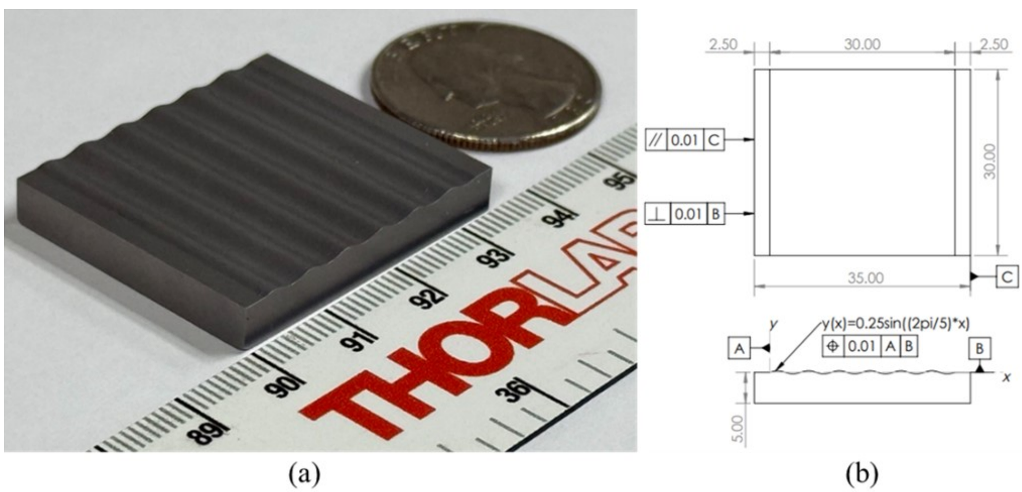

Fig. 4 NIST traceable target used to validate the sensor's measuring resolution: (a) image of the NIST traceable target with the designed sinusoidal surface profile; and (b) design drawing of the NIST traceable target, where the sinusoidal surface profile is defined by y(x) = 0.25sin(0.4πx).

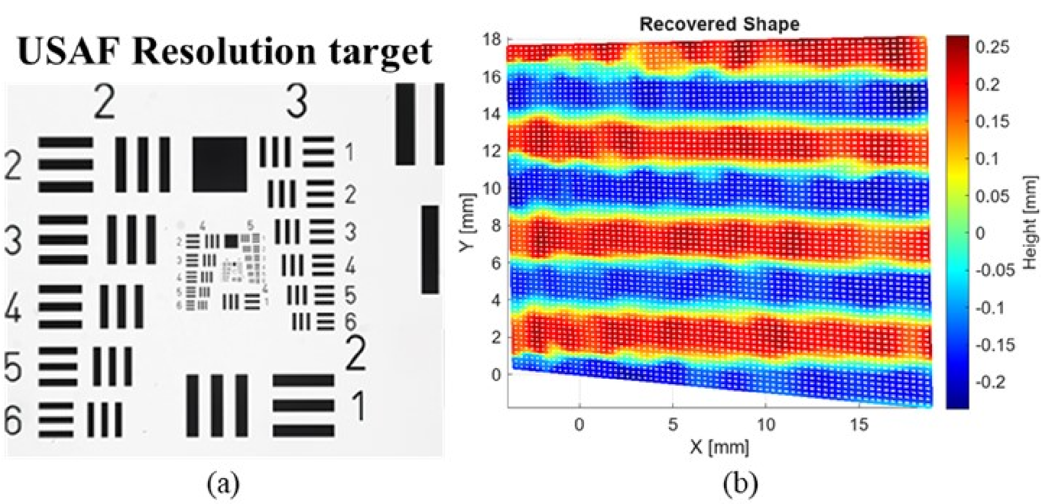

Fig. 5 Spatial and measuring resolution of the surface sensor: (a) image of a USAF target taken with the Basler daA1920-160um camera (50° FOV lens, 100 mm working distance); and (b) 3D reconstruction of the sinusoidal NIST traceable target. The spatial and measuring resolutions are approximately 62.5 μm and 50 μm, respectively.

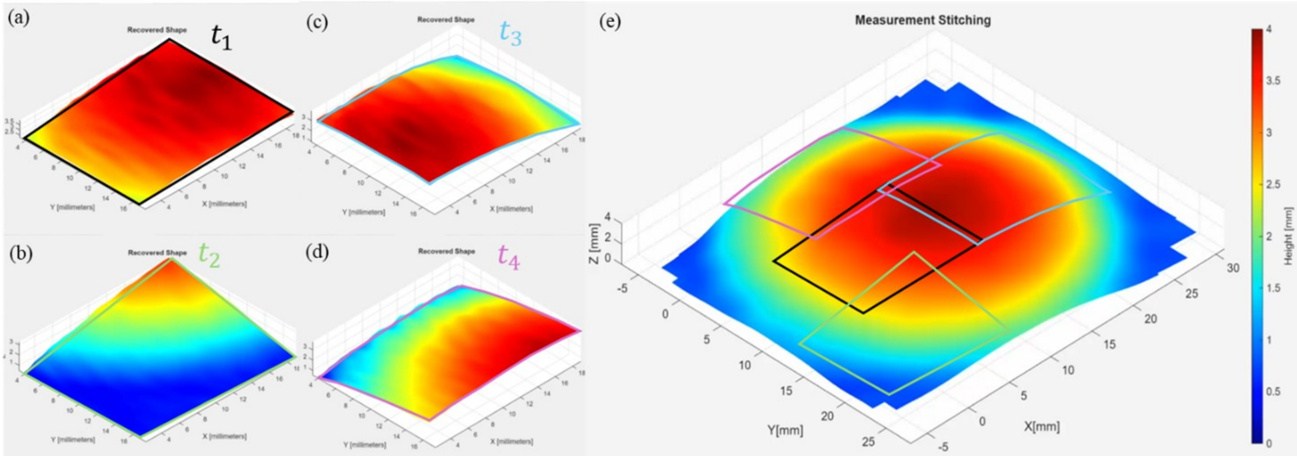

Fig. 6 Representative surface measurements taken at different time instances while the senor is subjected to 120 mm/s motion: (a)-(d) show small area surface measurements at four different time instances, each outlined in a different color; and (e) shows the stitched single-layer measurement, with colored outlines corresponding to the small area surface measurements in (a)-(d).

Conclusion and Future Works

The current results demonstrate the feasibility of the assembled testing platform in matching the actual AM processing parameters both dynamically and structurally. The miniaturized surface sensor utilizing FP methodology shows promising preliminary results in capturing depth information in motion and in real time. The single-layer stitching result indicates that the sensor is suitable for monitoring an AM part *in-situ*, during fabrication: as the part is built layer by layer, the sensor can record the depth information at each layer, ultimately forming a complete 3D digital representation of the finished part.

Future works will focus on improving the spatial and measuring resolution through advance filtering method and optimization of the observation and projection systems. Additional efforts will be placed on investigating composite shape recovery methods to augment the phase-to-height look-up table, since the look-up table method suffers from a limited measurements range [10]. By adding a coarse height estimation step before the look-up table, the effective measurement range can be increased significantly. Overall, the current developments serve as a starting point for optimizing a real-time surface sensor for *in-situ* AM applications and can be tailored to specific types of AM environments. It is envisioned that additional measurement capabilities, such as subsurface sensing and chemical analysis, can be integrated into the current sensor in the future to create a comprehensive and multimodal real-time, *in-situ* AM monitoring system.

Acknowledgments We sincerely acknowledge the Department of Energy for their generous sponsorship, which has been instrumental in the success of this project. Additionally, we extend our gratitude to our colleagues at the Center for Holographic Studies and Laser micro-mechaTronics (CHSLT) for their invaluable support and assistance throughout the research.

References

1. Chen, X., Xi, J.,Tao, J. and Ye, J., "Research and development of an accurate 3D shape measurement system based on fringe projection: Model analysis and performance evaluation," *Prec. Engg.*, *32*, pp. 215-221, 2008.
2. Ruiz-Cadalso, D. and Furlong, C., "Application of instantaneous polarization imagers for quantitative optical metrology by digital holography," *Proc., SEM 2024 Annu. Conf.*, 2024.
3. Takeda, M. and Mutoh, K., "Fourier transform profilometry for the automatic measurement of 3-d object shapes," *Appl. Opt.*, *22*(24), pp.3977-3982, 1983.
4. Huang, L., Qian, K., Pan, B. and Asundi, A., "Comparison of Fourier transform, windowed Fourier transform, and wavelet transform methods for phase extraction from a single fringe pattern in fringe projection profilometry," *Opt. Lasers Engg.*, *48*(2), pp. 141–148, 2010.
5. Ri. S., Fujigaki, M. and Morimoto, Y., "Sampling Moiré method for accurate small deformation distribution measurement," *Exp Mech*, *50*(4), pp. 501–508, 2010.
6. Zou, C., Huang, L., Zhang, M., Chen, Q. and Asundi, A., "Temporal phase unwrapping algorithms for fringe projection profilometry: A comparative review," *Opt. Lasers in Eng.*, *85*, pp. 84–103, 2016.

7. Zhao, M., Huang, L., Zhang, Q., Su, X., Asundi, A. and Kemao, Q., "Quality-guided phase unwrapping technique: comparison of quality maps and guiding strategies," *Appl. Opt., 50*(33), p. 6214, 2011.
8. Suzuki, S., Akatsuka, Y., Jiang, W., Fujigaki, M. and Otsu, M., "Development of quick three-dimensional shape measurement projection mapping system using a whole-space tabulation method," *Appl. Sci.*, *9*(20), p. 4408, 2019.
9. Zheng, H., Salerni, A. and Furlong, C., "Real-time surface metrology in-situ by dual-frequency fringe projection to augment smart manufacturing," *Proc., SEM 2024 Annu. Conf.*, 2024.
10. Guo, W., Wu, Z., Xu, R., Zhang, Q., and Fujigaki, M., "A fast reconstruction method for three-dimensional shape measurement using dual-frequency grating projection and phase-to-height lookup table." *Opt. Laser Technol.*, *112*, pp.269–277, 2019.